ME 614 Spring 2017- Final Project

Imcompressible Lid-driven Cavity Flow

Zitao He

05/05/2017

Lid Driven Cavity Flow Simulation using CFD & Python

Zitao He

Department of Mechanical Engineering, Purdue University

I. Introduction

The lid-driven cavity flow problem has been studied for many years as a benchmark case for the study of computational methods to solve Navier-Stokes equations. Fluid flow behaviours inside lid driven cavities have been the subject of extensive computational and experimental studies over the past years. In this problem, the side and bottom walls (boundaries) surrounding the cavity are fixed but the upper surface (lid) of the cavity is moved at a uniform velocity. Many investigators have solved this problem assuming an incompressible fluid inside the cavity. Applications of lid driven cavities includes material processing, dynamics of lakes, metal casting and galvanizing. In this work, staggered grid was implemented to couple velocity and pressure and solve lid-driven cavity flow problem. Runge-Kutta iteration method was used for time advancements. The results were compared with the data from the Ghia, et al. [1] and matched very well. This paper aims to provide a CFD simulation study of incompressible viscous laminar flow in cavity flow using Python package.

II. Problem description

The cavity flow problem is described in the following figure. Basically, there is a constant velocity across the top of the cavity which creates a circulating flow inside as shown in Fig 1. To simulate this there is a constant velocity boundary condition applied to the lid, while the other three walls obey the no slip condition. Different Reynolds numbers give different results, so in this article Re=100, and Re=1000 were applied. At high Reynolds numbers we expect to see secondary circulation zones forming in the corners of the cavity.

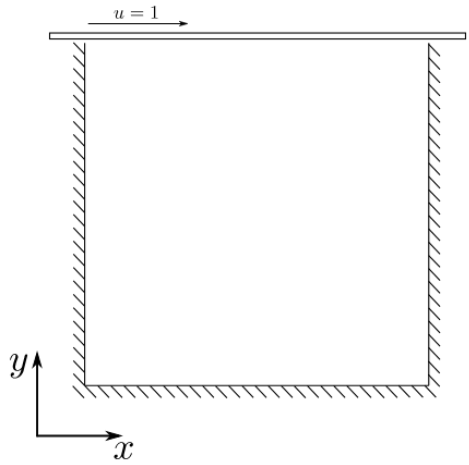

Fig. 1: Physical description of lid-driven cavity flow

Here is the system of differential equations(Navier-Stokes equations): two equations for the velocity components u, v, and one equation for pressure p:

$$\frac{\partial u}{\partial t} + u\frac{\partial u}{\partial x} + v\frac{\partial u}{\partial y} = -\frac{1}{\rho}\frac{\partial p}{\partial x} + \nu\left(\frac{\partial^2 u}{\partial x^2} + \frac{\partial^2 u}{\partial y^2}\right)$$
$$\frac{\partial v}{\partial t} + u\frac{\partial v}{\partial x} + v\frac{\partial v}{\partial y} = -\frac{1}{\rho}\frac{\partial p}{\partial y} + \nu\left(\frac{\partial^2 v}{\partial x^2} + \frac{\partial^2 v}{\partial y^2}\right)$$
$$\frac{\partial^2 p}{\partial x^2} + \frac{\partial^2 p}{\partial y^2} = -\rho\left(\frac{\partial u}{\partial x}\frac{\partial u}{\partial x} + 2\frac{\partial u}{\partial y}\frac{\partial v}{\partial x} + \frac{\partial v}{\partial y}\frac{\partial v}{\partial y}\right)$$

The initial condition is u,v,p=0; u,v,p=0 everywhere, and the boundary conditions are:

$$u = 1 \text{ at } y = 2 \text{ (the "lid");}$$

$$u, v = 0 \text{ on the other boundaries;}$$

$$\frac{\partial p}{\partial y} = 0 \text{ at } y = 0;$$

$$p = 0 \text{ at } y = 2$$

$$\frac{\partial p}{\partial x} = 0 \text{ at } x = 0, 2$$

III. Methodology

In this article, projection method was applied to calculate fields. The projection method is an effective means of numerically solving time-dependent incompressible fluid-flow problems. It was originally introduced by Alexandre Chorin in 1967 [2] as an efficient means of solving the incompressible Navier-Stokes equations. The key advantage of the projection method is that the computations of the velocity and the pressure fields are decoupled. The basics of staggered grid can be illustrated in Fig 2.

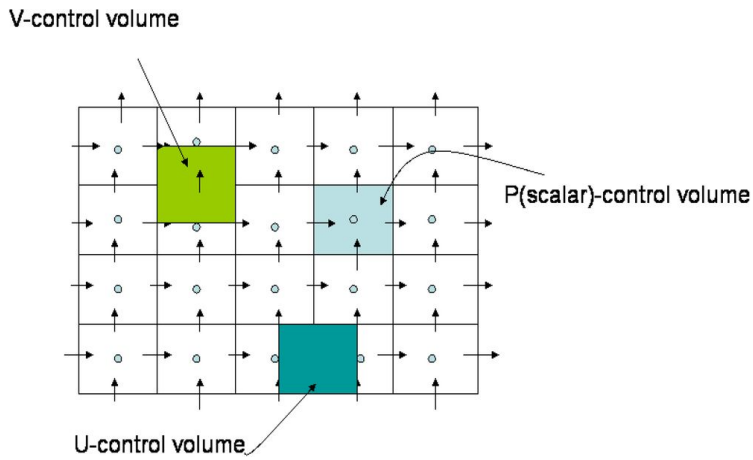

Fig. 2: Staggerd grid schematic[3]

For u-momentum equation, discretization was as follows:

$$\frac{u_{i,j}^{n+1} - u_{i,j}^{n}}{\Delta t} + u_{i,j}^{n}\frac{u_{i,j}^{n} - u_{i-1,j}^{n}}{\Delta x} + v_{i,j}^{n}\frac{u_{i,j}^{n} - u_{i,j-1}^{n}}{\Delta y}$$
$$= -\frac{1}{\rho}\frac{p_{i+1,j}^{n} - p_{i-1,j}^{n}}{2\Delta x} + \nu\left(\frac{u_{i+1,j}^{n} - 2u_{i,j}^{n} + u_{i-1,j}^{n}}{\Delta x^2} + \frac{u_{i,j+1}^{n} - 2u_{i,j}^{n} + u_{i,j-1}^{n}}{\Delta y^2}\right)$$

Similarly for the v-momentum equation:

$$\frac{v_{i,j}^{n+1} - v_{i,j}^{n}}{\Delta t} + u_{i,j}^{n}\frac{v_{i,j}^{n} - v_{i-1,j}^{n}}{\Delta x} + v_{i,j}^{n}\frac{v_{i,j}^{n} - v_{i,j-1}^{n}}{\Delta y}$$
$$= -\frac{1}{\rho}\frac{p_{i,j+1}^{n} - p_{i,j-1}^{n}}{2\Delta y} + \nu\left(\frac{v_{i+1,j}^{n} - 2v_{i,j}^{n} + v_{i-1,j}^{n}}{\Delta x^2} + \frac{v_{i,j+1}^{n} - 2v_{i,j}^{n} + v_{i,j-1}^{n}}{\Delta y^2}\right)$$

Finally, the discretized pressure-Poisson equation can be written as:

$$\frac{p_{i+1,j}^{n} - 2p_{i,j}^{n} + p_{i-1,j}^{n}}{\Delta x^2} + \frac{p_{i,j+1}^{n} - 2 * p_{i,j}^{n} + p_{i,j-1}^{n}}{\Delta y^2}$$
$$= \rho\left[\frac{1}{\Delta t}\left(\frac{u_{i+1,j} - u_{i-1,j}}{2\Delta x} + \frac{v_{i,j+1} - v_{i,j-1}}{2\Delta y}\right)\right.$$
$$-\frac{u_{i+1,j} - u_{i-1,j}}{2\Delta x}\frac{u_{i+1,j} - u_{i-1,j}}{2\Delta x} - 2\frac{u_{i,j+1} - u_{i,j-1}}{2\Delta y}\frac{v_{i+1,j} - v_{i-1,j}}{2\Delta x}$$
$$\left. -\frac{v_{i,j+1} - v_{i,j-1}}{2\Delta y}\frac{v_{i,j+1} - v_{i,j-1}}{2\Delta y}\right]$$

IV. Results and Validation

The contour plots for u, v, and p for Re = 100 and Re = 1000 were made to show the characteristics of the cavity flow. Re = 100 was taken for low Reynolds number. The results were shown in Fig 3 to Fig 6.

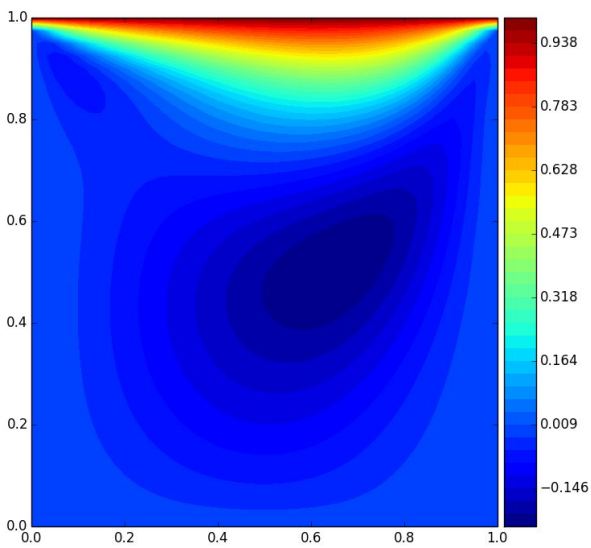

Fig. 3: Horizontal velocity distribution(Re = 100)

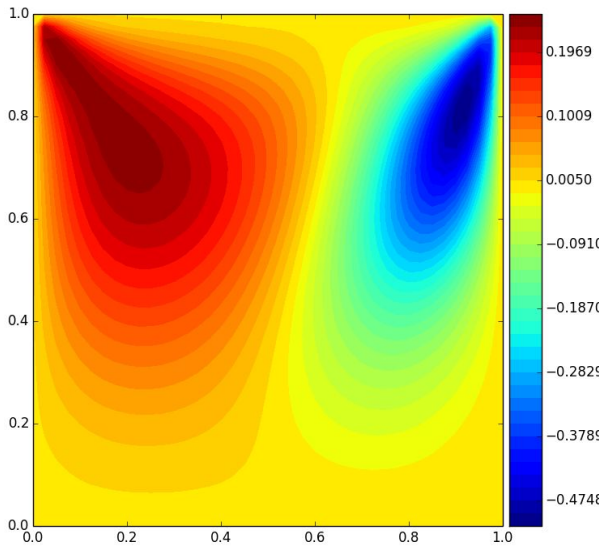

Fig. 4: Vertical velocity distribution(Re = 100)

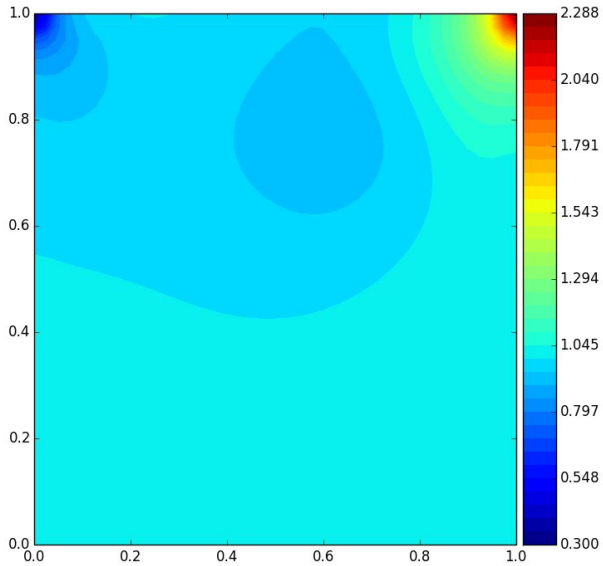

Fig. 5: Pressure distribution(Re = 100)

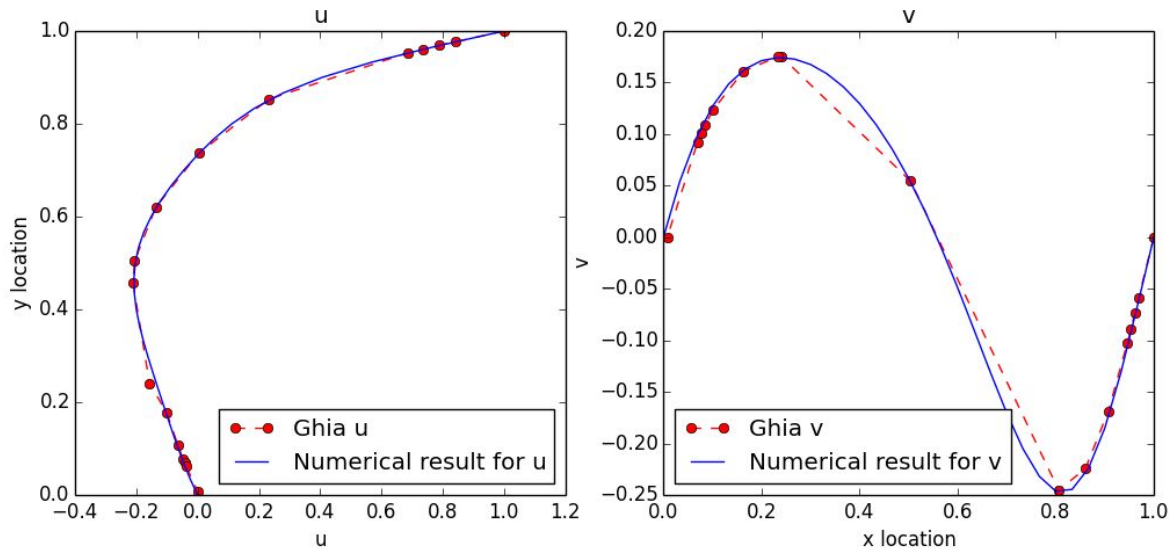

Fig. 6: Validation of u and v along cneterlines based on data from Ghia, et al. [1] (Re = 100)

The simulation results match to the data points from Ghia, et al. very well.

Re = 1000 was taken for high Reynolds number. The results were shown in Fig 7 to Fig 10.

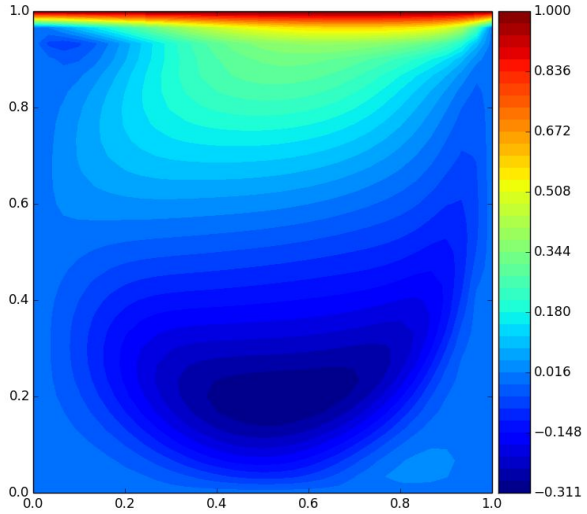

Fig. 7: Horizontal velocity distribution(Re = 1000)

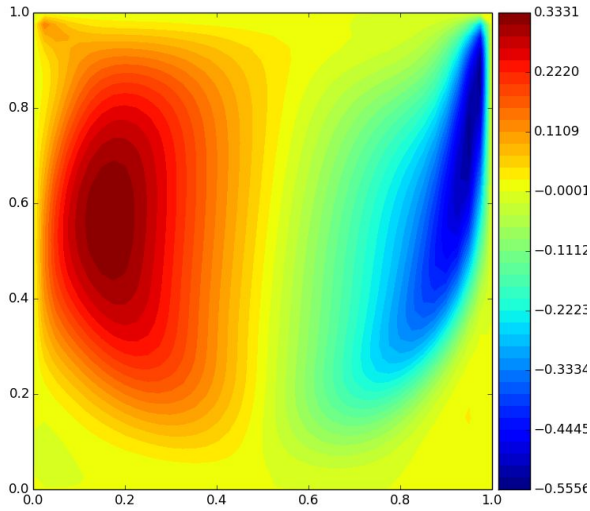

Fig. 8: Vertical velocity distribution(Re = 1000)

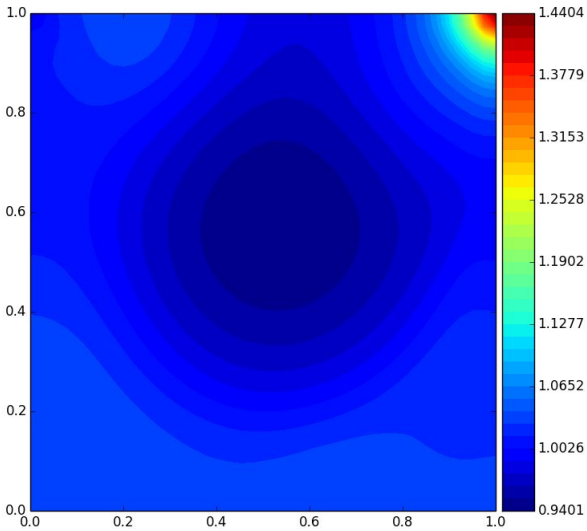

Fig. 9: Pressure distribution(Re = 1000)

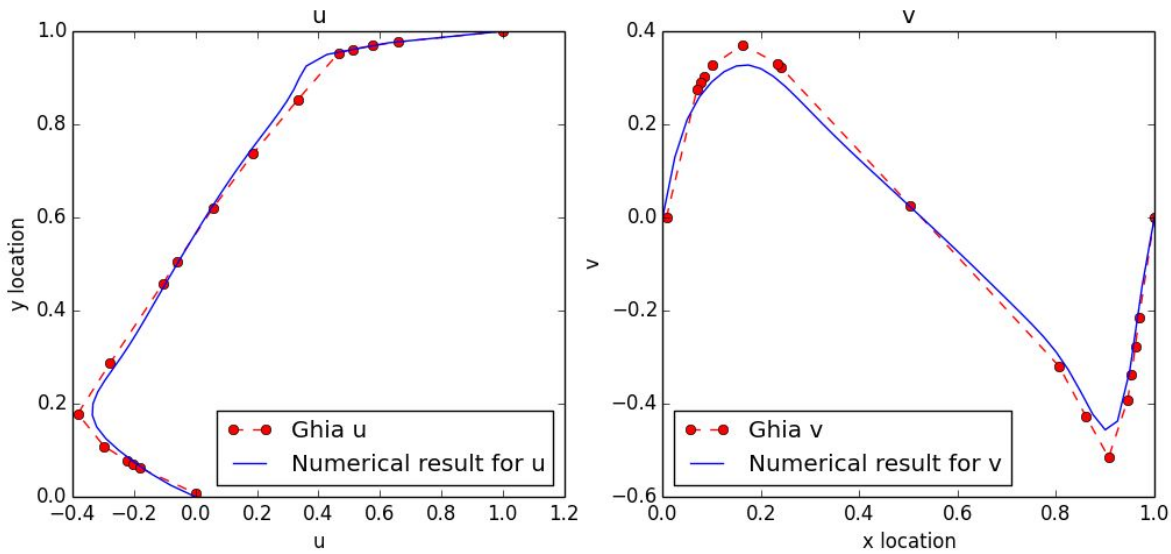

Fig. 10: Validation of u and v along cneterline based on the data from Ghia, et al. [1] (Re = 1000)

The contour plots for stream function and streamline plots for Re = 100 and Re = 1000 were made to show the characteristics of the cavity flow in Fig 11 and Fig 12 respectively.

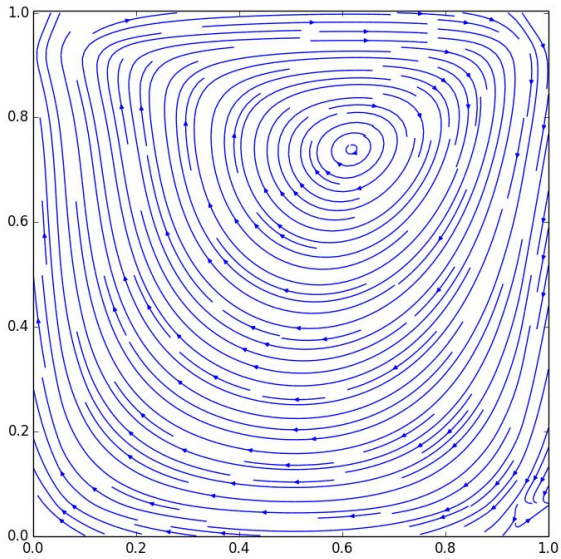

Fig. 11: Streamlines contour plot(Re = 100)

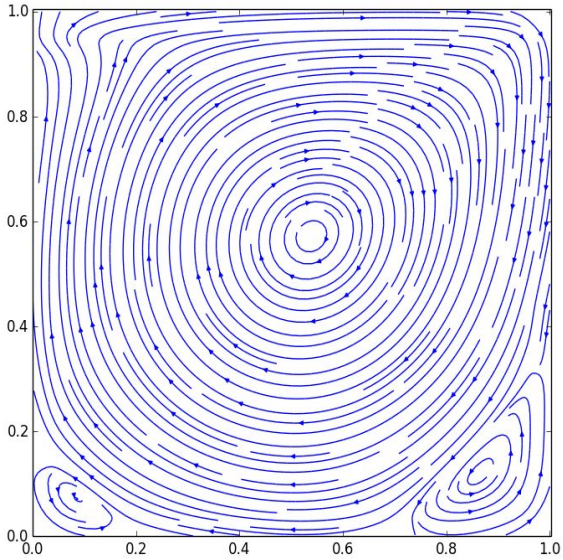

Fig. 12: Streamlines contour plot(Re = 1000)

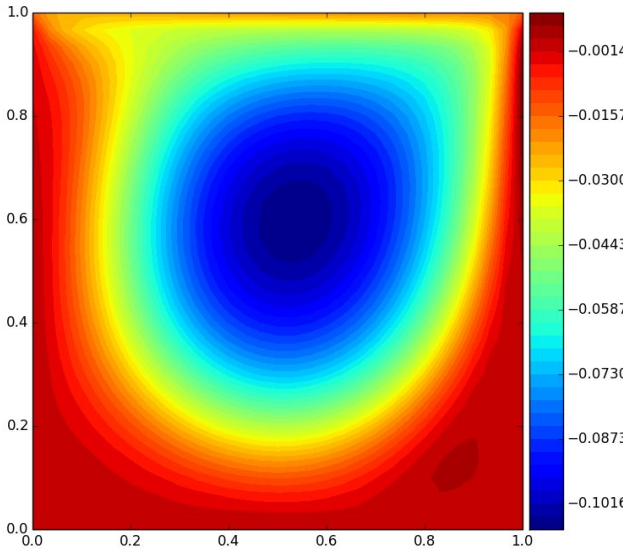

Fig. 13: Stream function contour(Re = 1000)

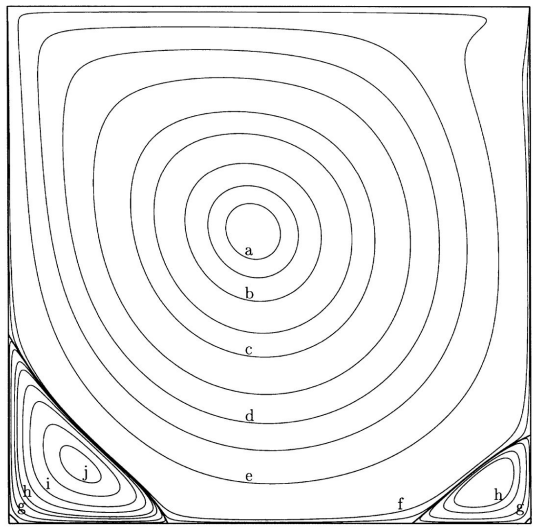

Fig. 14: Streamlines from Botella & Peyret (1998) [4]

	Streamfunction					
Value	0.1175	0.115	0.11	0.1	9×10^{-2}	7×10^{-2}
label	a		b		c	
Value	5×10^{-2}	3×10^{-2}	1×10^{-2}	1×10^{-4}	1×10^{-5}	1×10^{-10}
label	d		e	f		
Value	0.0	-1×10^{-6}	-1×10^{-5}	-5×10^{-5}	-1×10^{-4}	-2.5×10^{-4}
label			g		h	
Value	-5×10^{-4}	-1×10^{-3}	-1.5×10^{-3}			
label	i		j			

Table 1. The value and the corresponding label of the streamfunction contours in Botella & Peyret (1998)

In the comparison of u and v value along centerlines, the data matches to each other well except for the peak value. This might happen when Reynolds number is high enough to bring error in.

Stream function from numerical simulation and stream function contour from Botella & Peyret (1998)[4] match to each other quantitatively as shown in Fig 13 and Fig 14. The largest value is around 0.11(deep blue area) and the lowest value is almost zero(deep red area). There are two areas on the two bottom corners where the stream function value is a little bit above zero. This is caused by the secondary flows due to high Reynolds number for this case.

It is needed to mention that the velocity of the lid in this numerical simulation(u = 1 m/s) is opposite to the velocity adopted in Botella & Peyret (1998) (u = -1 m/s) which make the contour plot symmetric along y direction for two plots. In addition, the secondary flows in Fig. 11 and Fig. 12 are recognizable, however, in the stream function plot (Fig. 13), the secondary areas are not apparent enough. This is due to limited mesh quality and convergence criteria. To get better results, mesh quality should be increased and time step dt should be decreased.

V. Discussion and conclusions

In this work, numerical solutions with staggered grid and fully explicit time discretization were obtained for laminar flow inside a square cavity of which lid moves at variable velocity and analytical solution is known (Ghia, et al, 1982 and Botella & Peyret, 1998). The authors use a vorticity-stream function formulation of the 2D N-S Momentum Equations with a coupled strongly implicit multigrid method.

Velocify field was plotted along centerlines. Results were also presented in the way of colorful contour plots to compare with the existed publications.

This project was the summary of what was learnt in this course during this semester. We started with the 1-D spatial discretization and moved toward the more complicated problems such as pressure Poisson equation solver and parallel computation implementation on CFD. The last homework was particularly helpful in finding the solutions of this project which introduces the ideas about how to code with Navier-Stokes equations. This project closely resemble actual engineering problems and thus an important aspect of ME 614 Computational Fluid Dynamics.

VI. References

[1] Ghia, U. K. N. G., Ghia, K. N., & Shin, C. T. (1982). High-Re solutions for incompressible flow using the Navier-Stokes equations and a multigrid method. Journal of computational physics, 48(3), 387-411.

[2]Chorin, A. J. (1967). The numerical solution of the Navier-Stokes equations for an incompressible fluid. Bulletin of the American Mathematical Society, 73(6), 928-931.

[3] Babarinsa, O., Ogedengbe, E. O., & Rosen, M. A. (2014). Mixing Performance of a Suspended Stirrer for Homogenizing Biodegradable Food Waste from Eatery Centers. Sustainability, 6(9), 5554-5565.

[4] Botella, O., & Peyret, R. (1998). Benchmark spectral results on the lid-driven cavity flow. Computers & Fluids, 27(4), 421-433.